 doi:10.20944/preprints201806.0141.v1

Gambogenic Acid Triggers Apoptosis of Human Nasopharyngeal Carcinoma CNE-2Z Cells through Activating Volume-Sensitive Outwardly Rectifying Chloride Channels

Jingjing Su[1, †], Ting Xu[1, †], Genling Jiang[2], Mengru Liang[1], Hui Cheng[1], Mei Hou[1], Qinglin Li[1,*]

[1]Key Laboratory of Xin'an Medicine, Ministry of Education, Anhui Province Key Laboratory of R&D of Traditional Chinese Medicine, Anhui University of Chinese Medicine, Hefei, 230038, China;

[2]Anhui New Star Pharmaceutical Development Co., Ltd, Hefei, 230038, China;

[†]These authors contributed equally to this work.

[*]Corresponding author: Qinglin Li, Department of Experimental Center for Scientific Research, Anhui University of Chinese Medicine, Hefei, 230038, China. Tel.:+86-551-65169371; Fax: +86-551-65169371. E-mail address: liqinglin@ahtcm.edu.cn.

Abstract

Nasopharyngeal carcinoma (NPC) has not been thoroughly studied, and the pathogenesis of NPC is unclear. Scientists have neither discovered effective therapies nor achieved a desirable prognosis. Some studies have found that the regulation of intra- and extracellular ion channels hinges directly on cell apoptosis, and treatment with

 doi:10.20944/preprints201806.0141.v1

Gambogenic acid (GNA) brings changes to the volume-sensitive outwardly rectifying chloride (VSOR Cl^-) current of CNE-2Z cells recorded by the patch clamp method. Nevertheless, rarely have any researchers probed into the relevance between this variation and the anti-tumor mechanism of GNA. This paper is suggested that GNA activates the VSOR Cl^- current on the CNE-2Z cell membrane, and the activation of VSOR Cl^- currents by GNA in CNE-2Z cells is blocked by the chloride channel blockers DIDS and DCPIB. GNA induces the down-regulation of GRP78 and up-regulation of ATF4 as well as chop proteins, which is evidence for the induction of CNE-2Z cell apoptosis, and this correlates with ER stress. GNA can activate the VSOR Cl^- channel and lead to the occurrence of ER stress, thus inducing the apoptosis of CNE-2Z cells and inhibiting the proliferation of CNE-2Z cells.

Keywords: Gambogenic acid; apoptosis; CNE-2Z cells; volume-sensitive outwardly rectifying chloride

1. Introduction

As one of the most common cancers in southern China and southeast Asia, nasopharyngeal carcinoma (NPC) poses severe health problems in southern China with an annual incidence of 15-50 cases per 100,00 individuals [1]. With the popularity of intensity-modulated radiation therapy and concurrent chemo-radiation therapy, much improvement has been made in the local and regional control of NPC for patients with

 doi:10.20944/preprints201806.0141.v1

locoregionally advanced diseases. However, the prognosis is still undesirable due to recurrence and distant metastasis [2]. Highly invasive in the late stages, NPC is rarely detected during regular medical examinations due to its unique location and lack of specific symptoms [3]. The carcinogenesis of NPC is thought to be associated with the complex interaction of genetic, viral, environmental, and dietary factors. The molecular pathogenesis of NPC includes altering the expression and function of multiple genes (e.g., dominant oncogenes, recessive oncogenes or tumor-suppressor genes) and the signaling pathways [4]. Further elucidation of the molecular mechanism underlying NPC is essential to the development of new effective therapeutic agents.

The ER function of perturbation response is critical to the survival of cells. The unfolded and misfolded proteins in the ER lumen accumulate under a number of cellular stress conditions, including nutrient deprivation, oxidative stress, hypoxia, glycosylation alteration, and calcium flux disturbance, and subsequently lead to alleged ER stress. Due to the activation of the unfolded protein response (UPR) in the stressed cells, ER stress results from the perturbation of the ER function or homeostasis. The UPR is primarily transduced by three ER-resident sensor proteins, including protein kinase R–like ER kinase, activating transcription factor 6α, and inositol requiring enzyme 1α. Lately, the URP has been repeatedly demonstrated as an important necessity for tumor cells to maintain malignancy and therapy resistance [5]. Under continued and severe ER stress, the UPR induces cell-death programs, thereby dispelling the stressed cells. With the accumulation of unfolded proteins, the ER chaperone protein of immunoglobulin

 doi:10.20944/preprints201806.0141.v1

heavy-chain-binding protein (GRP78) is increasingly expressed and dissociated from the ER receptors. This process activates the receptors and triggers ER stress response. ATF4 protein has shown to be more heavily present in cancer tissue than in normal tissue, and it is up-regulated by tumor microenvironment signals such as oxidative stress, hypoxia/anoxia and ER stress [6]. In response to ER stress, the expression of transcription factor CCAAT-enhancer binding protein homologous protein (CHOP), a major inducer of apoptosis, also increases [7].

Chloride channels have been demonstrated to be the critical factor in regulation of the cell cycle and cell proliferation [8, 9]. There are mainly six types of chloride channels, belonging to the CLC superfamily of voltage-gated chloride channels. It has been reported that apoptotic stimuli, both mitochondrion-mediated intrinsic ones and death receptor-mediated extrinsic ones, can rapidly activate VSOR Cl^- conductance in various types of cells [10-12]. The VSOR Cl^- channel is the key to the occurrence of apoptosis by inducing apoptotic volume decrease (AVD), a major hallmark of cell apoptosis and an early prerequisite to apoptotic events. Observed soon after cell swelling, the regulatory volume decrease (RVD) is completed by parallel activation of the VSOR Cl^- channels in numerous cell types [13, 14]. In addition, non-swelling-coupled activation of the VSOR Cl^- channels is believed to cause AVD in many cells[15, 16]. The prevention of AVD in various types of cells helps to evade subsequent biochemical and morphological apoptotic events and rescue cells from death [17, 18]. According to previous studies, the inhibition of the VSOR Cl^- channels could suppress the apoptotic events [19, 20].

 doi:10.20944/preprints201806.0141.v1

Gamboge is the dry resin of *Garcinia hanburyi* HOOK. f. (Guttiferae) with various bioactivities, including detoxifying, homeostasis maintaining, anti-inflammatory and parasiticidic. Available evidence suggests that gamboge bears anticancer characteristics, with GNA being its main component. In recent years, our lab has conducted related research on the anticancer effects of GNA. The results show that GNA can inhibit a variety of tumor cells, such as HT-29, K562, A549 [21], CNE-1 [22], HepG-2 [23], U251 [24] and HeLa [25] to name a few. Our previous studies manifested that GNA inhibits CNE-1 cell growth and proliferation, and it induces apoptosis [22]. The existing evidence indicates that the VSOR Cl^- channel has an effect on NPC. Although some studies have shown the variation in drug action on the VSOR Cl^- current in NPC [26], further exploration is necessary to reveal the mechanism of VSOR Cl^- channel-induced NPC cell apoptosis. This paper hypothesizes that the VSOR Cl^- channel is involved in GNA-induced apoptosis of CNE-2Z cells. To confirm this hypothesis, the VSOR Cl^- currents in CNE-2Z cells treated with GNA are investigated, and the potential signaling mechanism in the development of GNA-induced apoptosis in CNE-2Z cells is also discussed.

2. Materials and Methods

2.1. Drugs and Reagents

GNA (>99.0%) was purified using HPLC by Dr. X. Wang at the Anhui University of Chinese Medicine. Purified GNA was dissolved in RPMI 1640 (GIBCO, NY) and was

Preprints (www.preprints.org) | NOT PEER-REVIEWED | Posted: 8 June 2018 doi:10.20944/preprints201806.0141.v1

kept at -20 ℃. GNA was diluted as needed in complete culture medium immediately before use. N-[Ethoxycarbonylmethyl]-6-methoxyquinolinium bromide (MQAE) was from the Beyotime Institute of Biotechnology (Shanghai, China). 4′,6-Diamidino-2-phenylindole dihydrochloride (DAPI) was purchased from Sigma-Aldrich (St. Louis, MO, USA). The annexin V-FITC/propidium iodide apoptosis detection kit was from Bestbio (Beijing, China). The primary antibodies for GRP78, CHOP, and ATF4 were obtained from Cell Signaling Technology (Beverly, MA, USA). The β-actin antibodies were from Bioworld (Bioworld Technology, MN, USA). The ClC-3 antibodies were from Alomone Labs Ltd. (Jerusalem, Israel). ClC-3 siRNA was from GenePharma (Shanghai, China). Chemiluminescent ECL reagent was from the Millipore Co. (Billerica, MA, USA). Blue Basic Autorad Film was from ISC Bioexpress (Kaysville, UT, USA). 4,4'-Diisothiocyano-2,2'-stilbenedisulfonic acid (DIDS), the anion exchange inhibitor, and 4-(2-butyl-6,7-dichloro-2-cyclopentylindan-1-on-5-yl) oxybutyric acid (DCPIB), the volume-sensitive anion channel inhibitor, were from Promega Biotec (Madison, WI, USA) and Santa Cruz (CA, USA), respectively. All other common chemicals were from Amersco (NY, USA) or Keygen Biotechnology (Nanjing, China).

2.2. Cell culture

CNE-2Z (the poorly differentiated human nasopharyngeal carcinoma cell line) was purchased from ATCC. The CNE-2Z cells were routinely cultured in RPMI 1640 medium

Preprints (www.preprints.org) | NOT PEER-REVIEWED | Posted: 8 June 2018 doi:10.20944/preprints201806.0141.v1

with 10% newborn calf serum, 100 IU/ml penicillin and 100 μg/ml streptomycin in a humidified atmosphere of 5% CO_2 and 95% air at 37 °C. The cells were subcultured every 48 h.

2.3. Determination of the cell viability

The cell viability was assessed by the MTT assay. CNE-2Z cells were plated into 96-well culture plates at a density of 5×10^4 /well (100 μl). Experiments were performed in triplicate in a parallel manner for each concentration of GNA for different times, and then, MTT was added to each well to give a final concentration of 0.5 mg/ml, followed by incubation of the cells for 4 h at 37 °C. The formazan crystals were dissolved in dimethyl sulfoxide (DMSO, 150 μl/well). The absorbance was detected at 490 nm using a microplate reader.

2.4. Path-clamp experiments

The osmolarity of the isotonic perfusion solution was 300 mOsmol/L, and it was comprised of the following (mM): 70 NaCl, 0.5 $MgCl_2$, 2 $CaCl_2$, 10 HEPES and 140 D-mannitol. The osmolarity of the hypotonic perfusion solution was 160 mOsmol/L (47% hypotonic, compared to that of the isotonic solution), and it was comprised of the following (mM): 70 NaCl, 0.5 $MgCl_2$, 2 $CaCl_2$ and 10 HEPES. The pipette solution was comprised of the following (mM): 70 N-methyl-D-glucamine chloride (NMDG-Cl), 1.2 $MgCl_2$, 10 HEPES, 1 EGTA, 140 D-mannitol and 2 ATP, and its osmolarity was adjusted to

 doi:10.20944/preprints201806.0141.v1

300 mOsmol/L. The pH values of the perfusion and pipette solutions were adjusted to 7.4 and 7.25, respectively.

Whole cell currents were recorded with the EPC-10 patch clamp amplifier (HEKA EPC-10, Germany). The membrane potential was held at the Cl^- equilibrium potential (0 mV) and stepped up to 200 ms pulses of ±80, ±40 and 0 mV in sequence repeatedly, with 4 s intervals between pulses. The voltages and currents were recorded by using a laboratory interface. Currents were measured at 10 ms after the onset of the voltage steps.

2.5. Determination of the intracellular chloride ion concentration

The Krebs-HEPES buffer solution was comprised of the following (mM): 20 HEPES, 128 NaCl, 1 $MgCl_2$, 2.7 $CaCl_2$, 2.5 KCl, and 16 glucose, and its pH was adjusted to 7.4. The chloride ion fluorescent probe MQAE was excited at a wavelength of 355 nm, and emitted light was collected at a wavelength of 460 nm.

The fluorescence intensity of the probe was inversely proportional to the chloride ion concentration. A chloride ion fluorescent probe was used to detect and analyze the chloride channel activity of CNE-2Z cells prior and subsequent to mechanical stimulation. The CNE-2Z cells were placed in 48-well plates and treated with drugs for 24 h. The medium was replaced with culture medium containing 10 mM MQAE, and the cells were cultured in a 37 ˚C incubator for 1 h. The cells were rinsed with Krebs-HEPES buffer solution for 5 min 5 times, and the intra-cellular MQAE fluorescence was observed with a fluorescence microscope. For the densitometric analysis, 5 cells were

Preprints (www.preprints.org) | NOT PEER-REVIEWED | Posted: 8 June 2018 doi:10.20944/preprints201806.0141.v1

randomly selected from each group, and their fluorescence intensity was measured on the inverted digital images using Image J software.

2.6. DAPI staining experiment

The CNE-2Z cells were placed in 6-well plates and treated with drugs for 24 h. Cells in each well were stained with DAPI and photographed using a fluorescence microscope as previously described.

2.7. Annexin V/propidium iodide staining experiment

CNE-2Z cells were incubated with drugs for 24 and 48 h. After incubation, both floating and adherent cells were collected and washed once with phosphate-buffered saline (PBS). Cells were stained with FITC-annexin V (AV) and propidium iodide (PI), and the percentage of AV/PI-positive cells was calculated as previously described.

2.8. Transfection of CNE-2Z cells with ClC-3 siRNA

The siRNA against the human ClC-3 gene was marked with 5-FAM, and it was synthesized by the Shanghai GenePharma Company. The sequence of the ClC-3 siRNA was 5′-CAAUGGAUUUCCUGUCAUATT-3′, and its complementary strand was 5′-UAUGACAGGAAAUCCAUUGTA-3′. The sequence of the negative control siRNA was 5′-UUCUCCGAACGUGUCACGUTT-3′, and its complementary strand was 5′-ACGUGACACGUUCGGAGAATT-3′. The siRNAs were transfected with HiPerFect Reagent™ to a final concentration of 100 nM, following the manufacturer's instruction. The cells were further incubated in the normal growth conditions for 48 h or more before the experiments.

Preprints (www.preprints.org) | NOT PEER-REVIEWED | Posted: 8 June 2018 doi:10.20944/preprints201806.0141.v1

The transfection efficiency of siRNAs was tested by fluorescence microscopy and flow cytometry. After transfection with siRNA ClC-3 for approximately 6–24 h, the cells were cleaned with PBS three times. Cell images were then taken under a fluorescence microscope. The fluorescence intensities of the control and transfected cells were further analyzed by a flow cytometer using an excitation wavelength of 488 nm. The transfection efficiency was obtained by analyzing the fluorescence intensity of individual cells using flow cytometry.

2.9. Western blot analysis

CNE-2Z cells were washed with ice-cold PBS 3 times and bathed in RIPA lysis buffer with 1% PMSF for 30 min. Proteins were separated with 10% SDS-PAGE (for GRP78, ATF4, and CHOP) and transferred to nitrocellulose membranes. Membranes were incubated with primary antibodies at 4°C overnight, rinsed with PBST for 10 min 3 times, and then incubated with the secondary antibody at room temperature for 2 h. An ECL chemiluminescence kit was used, followed by detection by the gel analysis system. For the densitometric analysis, the optical density was measured on the inverted digital images using Alpha View SA software.

2.10. Statistical Analysis

All the experiments were repeated at least three times. The data were analyzed using the statistical software SPSS 13.0 and expressed as the mean ± standard error (S.E.). The significant differences were determined using the ANOVA test for multiple group comparisons. $P < 0.05$ was considered statistically significant.

Preprints (www.preprints.org) | NOT PEER-REVIEWED | Posted: 8 June 2018 doi:10.20944/preprints201806.0141.v1

3. Results

3.1. Effect of GNA on human NPC CNE-2Z cell viability

CNE-2Z cells were treated with GNA at various concentrations for 24 and 48 h. The MTT assay was used to detect cell viability. It was shown that GNA reduced the percentage of viable cells in a concentration- and time-dependent manner. The 50% inhibitory concentration (IC_{50}) values for CNE-2Z cells were 2.25 μM and 1.33 μM, respectively, at the various time points (24 h and 48 h) after GNA treatment (Fig. 1). Based on the estimated IC_{50} value for CNE-2Z cells, a concentration of 2 μM was therefore used in this study.

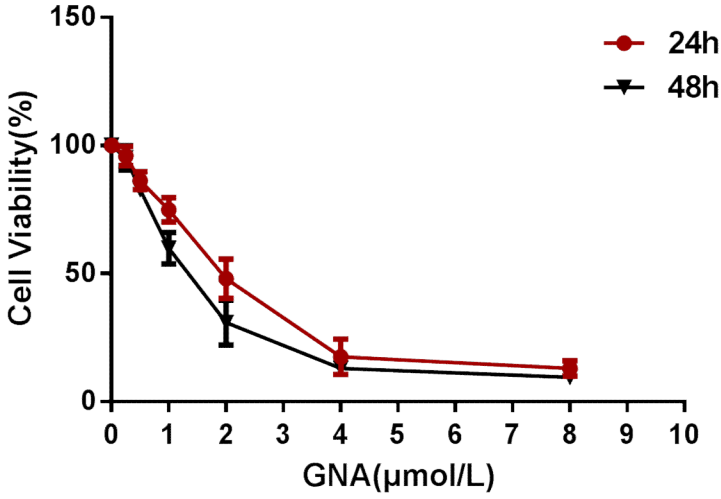

Fig. 1. Effects of GNA on the cell viability of CNE-2Z cells. GNA inhibits the growth and viability of CNE-2Z cells in the MTT assay. The cell survival rates in the experimental groups were decreased after treatment with GNA at doses of 0.25, 0.5, 1.0, 2.0, 4.0, and 8.0 μmol/L for 24 h or 48 h compared with the blank group. * $P<0.05$, ** $P<0.01$ versus the control.

Preprints (www.preprints.org) | NOT PEER-REVIEWED | Posted: 8 June 2018 doi:10.20944/preprints201806.0141.v1

3.2. GNA induces the apoptosis of CNE-2Z cells

Through the morphological observation of GNA-treated cells with an inversion microscope, it is noted that, compared to the control group, the cells of the GNA group became smaller, the nuclei suffered rupturing and apoptosis, and the number of apoptotic cells increased with increasing GNA concentrations (Fig. 2A). The results of the AV/PI assay demonstrate that the apoptosis rate is positively correlated with the GNA concentration (Fig. 2B).

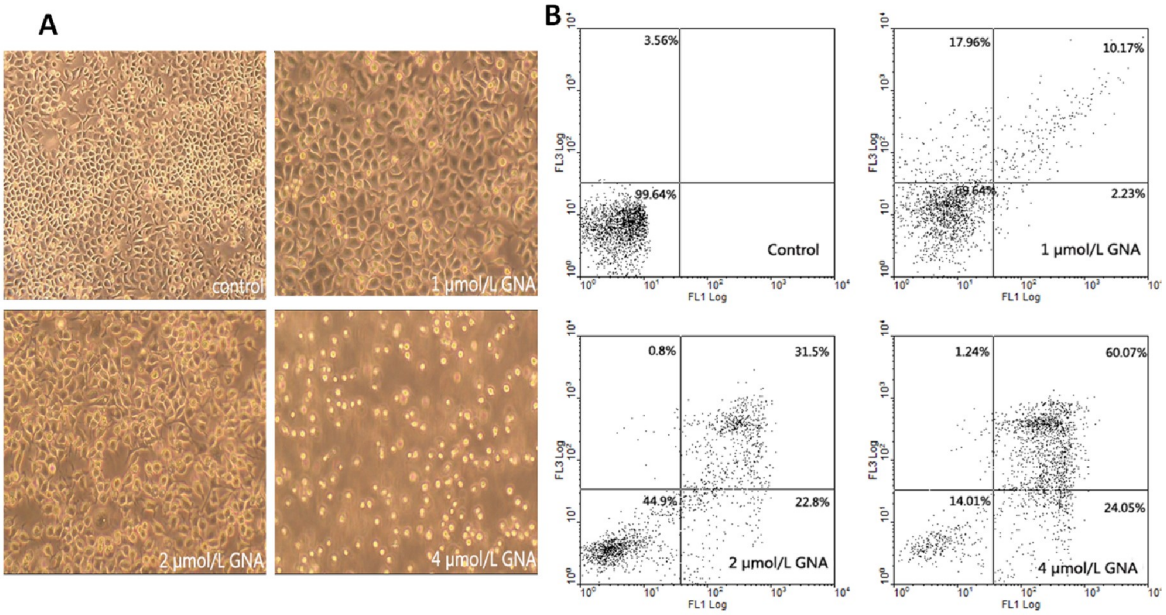

Fig. 2. Effects of GNA on the apoptosis of CNE-2Z cells. (A) The morphological changes of CNE-2Z cells after GNA treatment at different concentrations for 24 h. (B) Annexin V-FITV/PI double staining was used to detect the cell apoptosis rate after GNA treatment at different concentrations for 24 h by flow cytometry.

Preprints (www.preprints.org) | NOT PEER-REVIEWED | Posted: 8 June 2018 doi:10.20944/preprints201806.0141.v1

3.3. GNA rapidly activates VSOR Cl^- currents in CNE-2Z cells

The results illustrate that the background current of CNE-2Z cells is small and stable. Under the voltage clamp of -80 mV, an inward current is formed at the average current density of -4.9±0.5 pA/pF. When the voltage is clamped at +80 mV, an outward current is formed at the average current density of 4.3±0.8 pA/pF (Fig. 3). The perfusate is replaced with isotonic perfusion liquid containing continuous GNA flow. This replacement activates a current and prolongs the drug action. In this process, the current gradually increases, and it reaches the peak of the stable stage in 3 min. Under the fixed voltage clamp, in the last 100 ms, the inactivation of the current is dependent on the voltage and time. When the voltage is clamped at -80 mV, the current density for GNA activation is -7.4±0.9 pA/pF. When the voltage is clamped at 80 mV, GNA is activated at a current density of 13.0±0.5 pA/pF (Fig. 3). Therefore, the outward current is greater than the inward current, which has obvious advantages. Moreover, the GNA-induced chloride currents are markedly inhibited by the VSOR Cl^- blockers DIDS (Fig. 3A, 3-5 min, 43.4±4.3%, $P < 0.05$) and DCPIB (Fig. 3B, 3-5 min, 88.9±5.2%, $P < 0.05$).

Preprints (www.preprints.org) | NOT PEER-REVIEWED | Posted: 8 June 2018 doi:10.20944/preprints201806.0141.v1

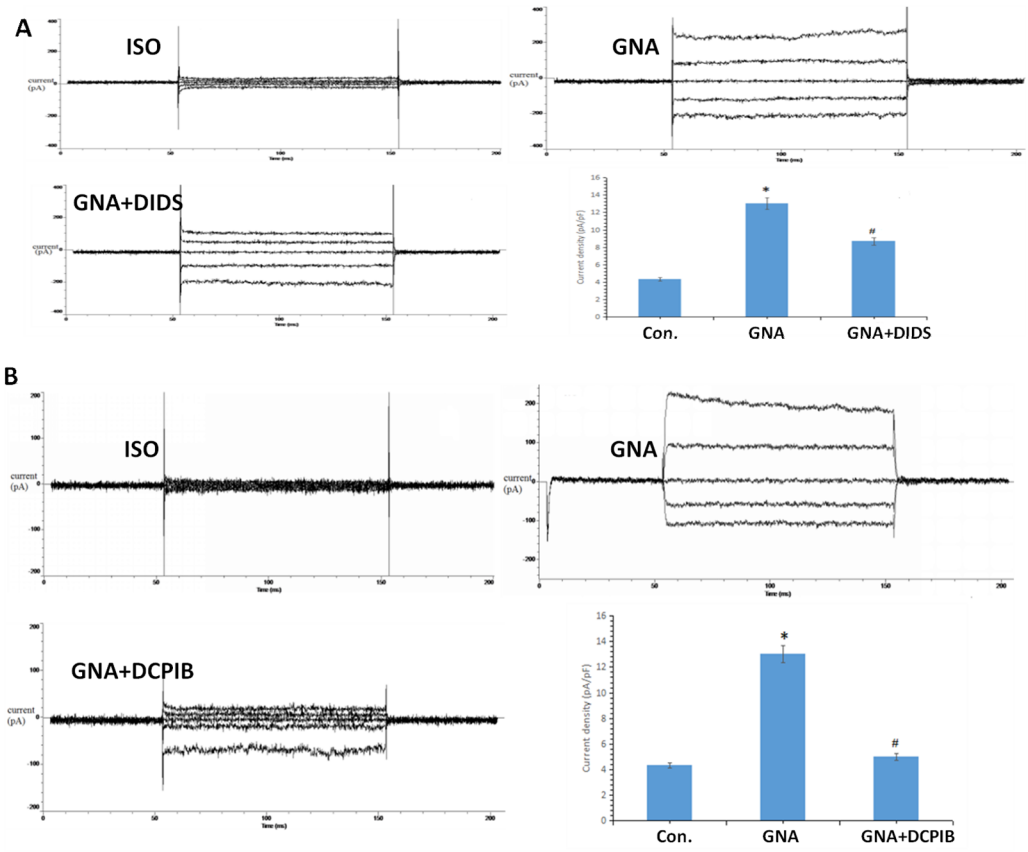

Fig. 3. Increased VSOR Cl^- currents of CNE-2Z cells after GNA treatment. (A) GNA-induced chloride currents were inhibited by adding DIDS (400 μmol/L). Current density at +80 mV. (B) GNA-induced chloride currents were inhibited by adding DCPIB (20 μmol/L). Current density at +80 mV. (C) Effects of GNA on the chloride ion concentration in CNE-2Z cells under a fluorescence microscope. CNE-2Z cells were treated with GNA in the presence or absence of DIDS or DCPIB for 24 h. Data in A, B and C represent the mean ± S.E. of five independent experiments. ** P <0.01 versus control; $^{\#\#}$ P<0.01 versus GNA.

3.4. Effect of GNA on the chloride concentration in CNE-2Z cells

Preprints (www.preprints.org) | NOT PEER-REVIEWED | Posted: 8 June 2018 doi:10.20944/preprints201806.0141.v1

After GNA treatment, the fluorescence intensity of MQAE is 74.7±5.3%, which is significantly higher than that of the normal control group. After DIDS treatment, the parameter is 47.9±1.8%, which is much lower than that of the GNA group. Similarly, the fluorescence intensity of MQAE (44.9±1.5%) after DCPIB treatment is obviously below that of the GNA group (Fig. 3C).

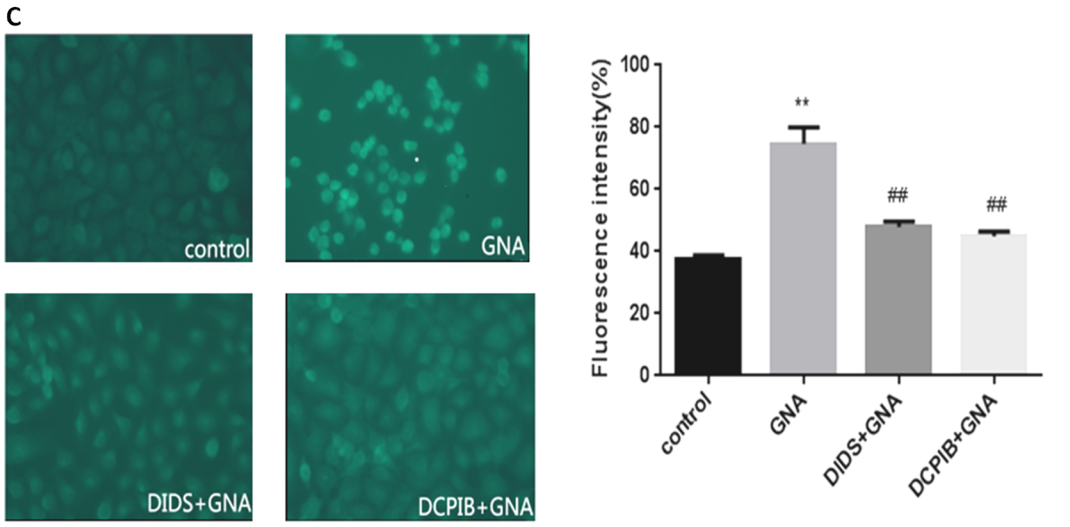

3.5. CLC-3 siRNA rescues NPC CNE-2Z cells from apoptosis

The siRNA technology is employed to specifically inhibit the expression of CLC-3 chloride channel proteins. To detect the transfection efficiency, CLC-3 siRNA is labeled with 5-FAM (green), and the fluorescence is monitored by a fluorescence microscope and a flow cytometer. As shown in Fig. 4A, fluorescence is detected in most of the cells treated with 100 nM 5-FAM-labeled ClC-3 siRNA 8 h after transfection, indicating that ClC-3 siRNA is successfully transfected into the cells. The transfection efficiency stands at 50%, as obtained through fluorescence intensity analysis of individual cells using flow cytometry (Fig. 4B).

Preprints (www.preprints.org) | NOT PEER-REVIEWED | Posted: 8 June 2018 doi:10.20944/preprints201806.0141.v1

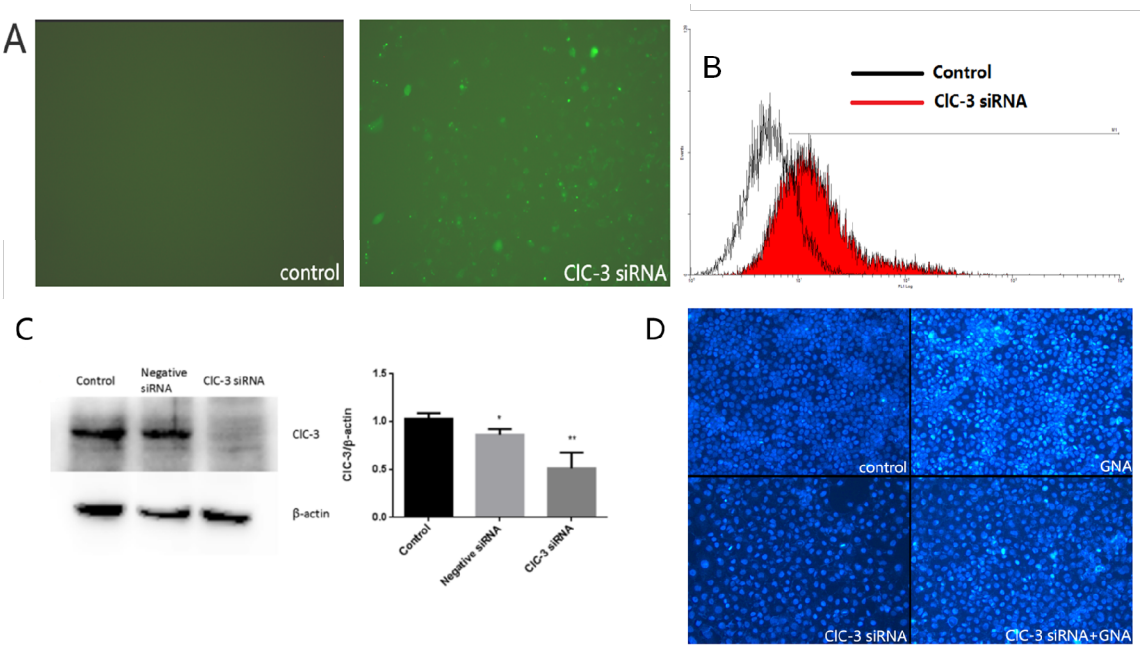

Fig. 4. Knockdown of the expression of ClC-3 chloride channels by ClC-3 siRNA in CNE-2Z cells. (A) Transfection efficiency of ClC-3 siRNA in CNE-2Z cells under a fluorescence microscope. The cells were transfected with ClC-3 siRNA labeled with 5-FAM (green) for 8 h. The green fluorescence was remarkably detected in the ClC-3 siRNA-treated cells, suggesting that the siRNA had been successfully transfected into the cells. (B) Transfection efficiency of ClC-3 siRNA in CNE-2Z cells detected by flow cytometry. M1 stands for the cells successfully transfected with the 5-FAM-labelled ClC-3 siRNA. (C) ClC-3 protein expression in CNE-2Z cells was detected by western blotting. Data represent the mean ± S.E. of three independent experiments. * $P<0.05$, ** $P<0.01$ versus the control. (D) DAPI staining was used to detect the cell apoptosis rate by a fluorescence microscope. CNE-2Z cells were treated with GNA in the presence or absence of ClC-3 siRNA for 24 h.

Preprints (www.preprints.org) | NOT PEER-REVIEWED | Posted: 8 June 2018 doi:10.20944/preprints201806.0141.v1

In order to determine the efficiency of ClC-3 knockdown, western blot techniques are adopted to detect the expression of the ClC-3 protein. The result shows that the expression of ClC-3 proteins is inhibited by ClC-3 siRNA (Fig. 4C).

This research further examines whether CLC-3 siRNA rescues NPC CNE-2Z cells from apoptosis. Through fluorescence microscopy, the cell volume shrinkage, typical nuclear chromatin condensation, and other morphological changes of apoptosis are observed after 2 μmol/L GNA exposure for 24 h by DAPI staining. These phenomena are evidence of the fact that CLC-3 siRNA reduces the morphological changes of apoptosis (Fig. 4D).

3.6. VSOR Cl^- channel blockers counteract ER stress-mediated CNE-2Z cell apoptosis

Previous studies have shown that gambogenic acid induces the apoptosis of CNE-2Z cells, and ERS has an effect on the apoptosis of CNE-1 and CNE-2 cells [23, 27]. Hence, the author tests the role of the VSOR Cl^- channel in ER stress-mediated CNE-2Z cell apoptosis with GNA. It is learned from the MTT assay that, after being treated with 2 μmol/L GNA for 24 h, the survival rate of CNE-2Z cells is lower than that of the control group. In the DIDS (400 μmol/L)+GNA (2 μmol/L) group and DCPIB (20 μmol/L)+GNA (2 μmol/L) group, the viabilities of the CNE-2Z cells are higher than that of the GNA group (Fig. 5A). Through fluorescence microscopy, the cell volume shrinkage, typical nuclear chromatin condensation, and other morphological changes of apoptosis are observed after DAPI staining. Therefore, GNA can inhibit the proliferation

Preprints (www.preprints.org) | NOT PEER-REVIEWED | Posted: 8 June 2018 doi:10.20944/preprints201806.0141.v1

of human NPC CNE-2Z cells, and the inhibition depends on both the time and concentration (Fig. 5B).

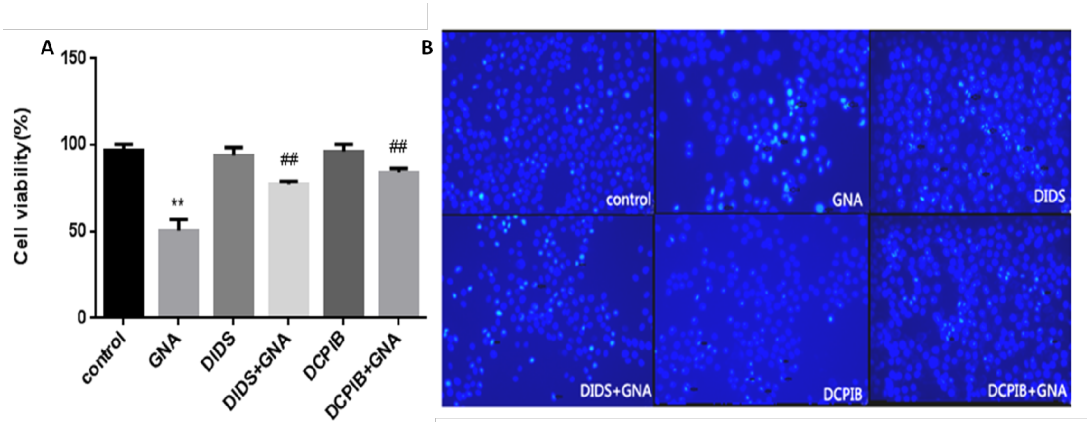

Fig. 5. Effects of DIDS (400 μmol/L) and DCPIB (20 μmol/L) on GNA-induced CNE-2Z cell death. CNE-2Z cells were treated with GNA in the presence or absence of DIDS or DCPIB for 24 h. Data represent the mean ± S.E. of three independent experiments. ** P<0.01, versus the control; $^{\#\#}$ P<0.01, versus GNA. (B) DAPI staining was used to detect the cell apoptosis rate under a fluorescence microscope. (C) Annexin V-FITV/PI double staining was used to detect the cell apoptosis rate under a fluorescence microscope. (D) Annexin V-FITV/PI double staining was used to detect the cell apoptosis rate by flow cytometry.

According to AV/PI double staining, the early apoptotic cell membrane is colored apple-green, while the late apoptotic or necrotic cytoplasm shows different levels of yellow-red color (Fig. 5C). The results of the AV/PI assay reveal that the apoptosis rate increases substantially when the cells are treated with 2 μmol/L GNA for 24 h. The

Preprints (www.preprints.org) | NOT PEER-REVIEWED | Posted: 8 June 2018 doi:10.20944/preprints201806.0141.v1

apoptosis of ER stress-mediated CNE-2Z cells is inhibited by DIDS and DCPIB (Fig. 5D).

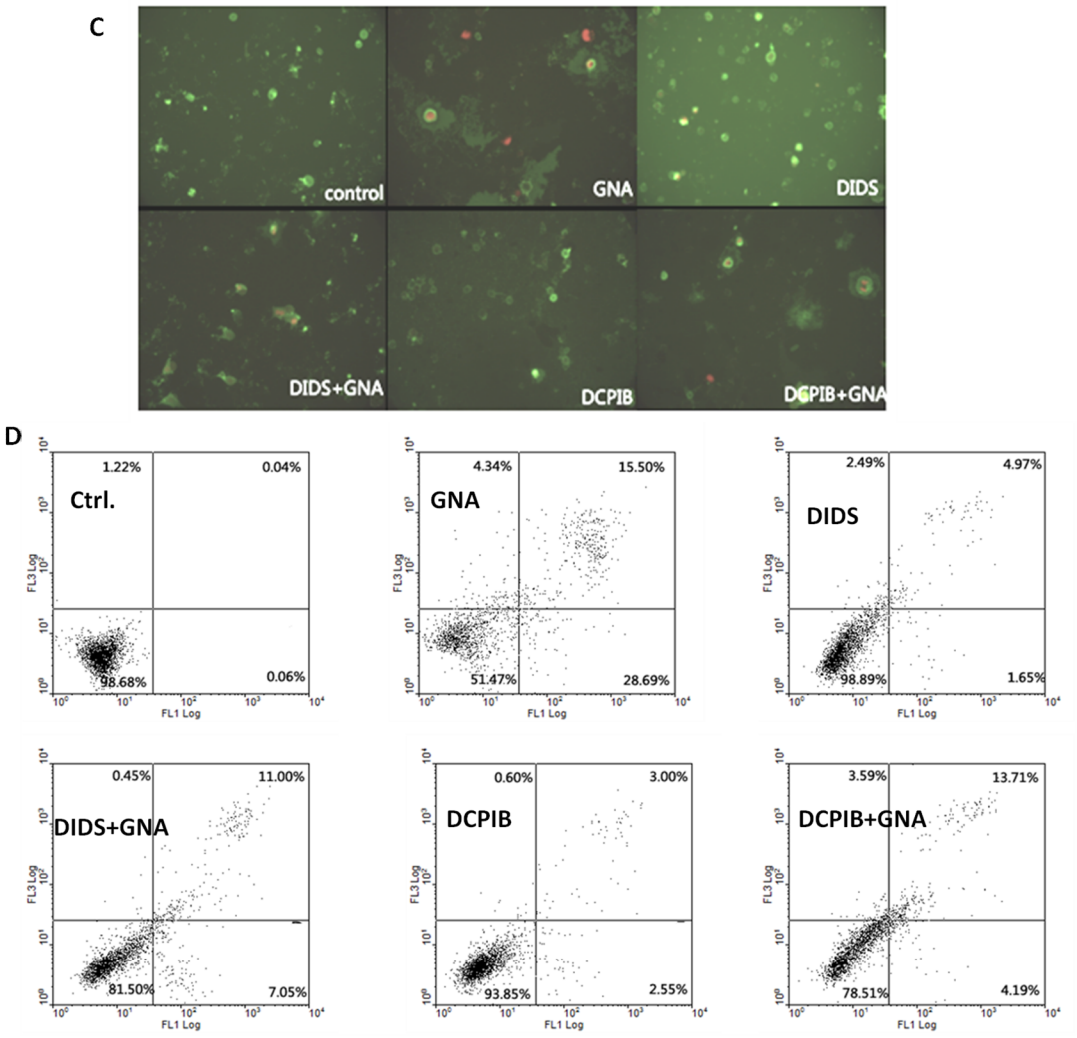

On this basis, CNE-2Z cells are treated with DIDS and DCPIB for 24 h to further explore whether the VSOR Cl^- channel mediates the apoptosis of CNE-2Z cells through ERS. The experimental results demonstrate that the expression of ER stress-related proteins, e.g., GRP78 protein, is down-regulated while the expression of ATF4 and CHOP proteins is up-regulated after 2 μmol/L GNA exposure for 24 h. In contrast, DIDS

Preprints (www.preprints.org) | NOT PEER-REVIEWED | Posted: 8 June 2018 doi:10.20944/preprints201806.0141.v1

and DCPIB significantly up-regulate GRP78 protein and down-regulate ATF4 and CHOP proteins (Fig. 6A, 6B, 6C).

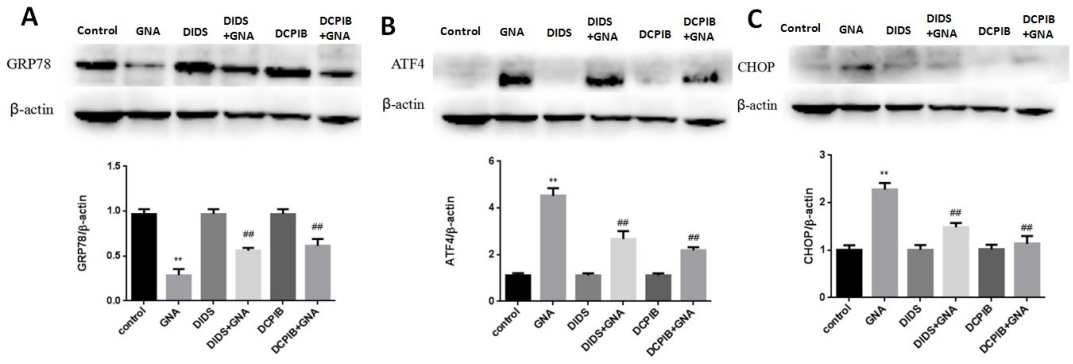

Fig. 6. Effects of DIDS or DCPIB on GRP78, ATF4 and CHOP protein expressions in CNE-2Z cells were detected by western blotting. (A-C) CNE-2Z cells were treated with GNA in the presence or absence of DIDS or DCPIB for 24 h. Data represent the mean ± S.E. of three independent experiments. ** $P<0.01$, versus the control; $^{\#\#}$ $P<0.01$, versus GNA.

4. Discussion

As suggested in the previous research, GNA is capable of inhibiting the cell diffusion of non-small cell lung cancer, gastric cancer, liver cancer, colon cancer and ovarian cancer [21, 28]. The curative effect and mechanism of GNA have been of wide concern.

Within a certain number of cells, the amount of MTT formation is positively correlated with the number of viable cells and enzyme marker, an indirect indicator of the number of viable cells and the absorbance. With the rise of the cell membrane permeability in apoptotic cells, the amount of DAPI in apoptotic cells increases. Coupled

Preprints (www.preprints.org) | NOT PEER-REVIEWED | Posted: 8 June 2018 doi:10.20944/preprints201806.0141.v1

with cell membrane damage, the variation in apoptosis and DNA structure causes ineffective discharge of the DAPI stain. The ensuing accumulation in the cell consequently leads to the higher fluorescence intensity of apoptotic cells than that of normal cells. In early apoptosis, PS, combined with AV, emits fluorescence and acts as a marker of apoptosis. However, PI cannot pass through the membrane of normal cells and early apoptotic cells but can pass through the membrane of the damaged and necrotic cells in late apoptosis. In association with the nucleus, PI enables the cells to give off red fluorescence. Therefore, AV is used in combination with PI to differentiate necrotic cells.

In this experiment, it is observed through fluorescence microscopy that the apoptotic cells are stained with bright blue by DAPI, and the surfaces of the early apoptotic cells are stained green by AV/PI. Meanwhile, the cytoplasm is not stained, and the cytoplasm of the late apoptotic/necrotic cells is dyed yellow-red with green surfaces. Flow cytometry shows that the apoptosis rate grows with increases in the GNA concentration, and it reaches approximately 50% when cells are treated with 2 mol/L GNA for 24 h. The results verify that GNA inhibits the proliferation of the NPC cell line CNE-2Z, and the inhibition effect is dependent on the concentration, time and induction of NPC CNE-2Z cell apoptosis.

In this study, the effect of GNA on the activation of chloride channels is measured by the patch clamp technique. In light of the experimental results, the extracellular perfusion with GNA activates a current with obvious outward dominance. The current direction is consistent with that of the chloride ions under different voltages. Besides,

Preprints (www.preprints.org) | NOT PEER-REVIEWED | Posted: 8 June 2018 doi:10.20944/preprints201806.0141.v1

DIDS or DCPIB inhibits the current. These effects are in good agreement with the literature [8], suggesting that the current may be VSOR Cl^- current. The concentration of intracellular ions is detected by a chloride-sensitive fluorescent indicator (MQAE) through the quenching of the fluorescence intensity of intracellular chloride ions. The results manifest the negative correlation between the fluorescence intensity of MQAE and the concentration of intracellular chloride ions. In addition, the fluorescence intensity of MQAE is increased after treatment with GNA, indicating that the concentration of intracellular chloride ions is decreased and the chloride ion channel is opened. Conversely, the fluorescence intensity of the cells declines with the addition of DIDS and DCPIB, a signal of the dramatic increase in the concentration of intracellular chloride ions. These results indicate that GNA promotes the opening of chloride ion channels and enlarges the efflux of chloride ions, while DIDS and DCPIB have the completely opposite effects. Patch clamp experiments prove that GNA activates the VSOR Cl^- current of the CNE-2Z cell membrane, and chloride channel blockers suppressed the activation of the VSOR Cl^- current of GNA-activated CNE-2Z cells. However, the VSOR Cl^- channel participates in the regulation of apoptotic volume reduction through mediating the transmembrane transport of chloride ions, which may be involved in the process of GNA-induced apoptosis in CNE-2Z cells.

The programmed cell death of apoptosis carries a series of morphological and biochemical characteristics, including cell shrinkage, the rapid increase of intracellular calcium, nuclear condensation, DNA fragmentation and the formation of apoptotic

Preprints (www.preprints.org) | NOT PEER-REVIEWED | Posted: 8 June 2018 doi:10.20944/preprints201806.0141.v1

bodies. Known as a shared feature of most cell apoptosis, the shrinking of cells or the decrease in the cell volume refers to the decrease of the apoptotic volume (apoptotic volume decrease, AVD). The AVD is regarded as an early trigger factor of apoptosis, as it emerges earlier than the release of cytochrome C, activation of cysteine aspartic protease (cysteine-containing aspartate-specific proteases, caspase-3) and fragmentation of DNA . The VSOR Cl^- current is activated in the mitochondria and by death receptor-mediated apoptosis, while the VSOR Cl^- channel blockers (NPPB and DIDS) can block the current, and they can turn tumor cells and T cells from apoptosis to recovery [29]. In accordance with previous data, the VSOR Cl^- channels play a very important role in the proliferation of human NPC, apoptosis of epithelial tumor cells and apoptosis of glomerular cells [30]. These results suggest that the VSOR Cl^- channel is engaged in the proliferation, metastasis and apoptosis of tumor cells. The ClC-3 chloride channel is a member of the voltage-dependent chloride channel family. When the cell volume increases, the ClC-3 channel is activated, and Cl^- efflux, the formation of chloride current, mediates the transport of substances, the release of intracellular organic matter and cell volume regulation. The ClC-3 channel protein is associated with cell proliferation, differentiation and apoptosis [30]. However, the molecular mechanism of VSOR Cl^- channel regulation is not clear, and the VSOR Cl^- channel protein is thought to be a P-glycoprotein (P-glycoprotein, P-gP), ClC-3 and ClC-2, which influences cell apoptosis by taking part in the regulation of the cell volume.

Preprints (www.preprints.org) | NOT PEER-REVIEWED | Posted: 8 June 2018 doi:10.20944/preprints201806.0141.v1

The VSOR Cl^- channel mediates the transmembrane transport of chloride ions to regulate the apoptotic volume decrease. Whereas it is worthwhile to study whether this channel partakes in GNA-induced apoptosis of CNE-2Z cells, GNA is used to induce the apoptosis of CNE-2Z cells in this research, the cells are treated with blocking agents (DIDS, DCPIB), and the survival rate of the cells, apoptosis and apoptosis rate are detected by MTT, DAPI staining and flow cytometry, respectively. It is observed that the chloride channel blockers (DIDS and DCPIB) effectively reduce the CNE-2Z-induced apoptosis of GNA cells. Then, the CLC-3 gene is silenced by a siRNA technique in CNE-2Z cells. The results reveal that the cell apoptosis after silencing the CLC-3 gene varies in a similar way to that of the apoptosis of CNE-2Z cells treated with blockers. Hence, the apoptosis of CNE-2Z cells induced by GNA may be related to the activation of the VSOR Cl^- channels, but the underlying mechanism still requires further exploration.

Previous studies have found that GNA induced CNE-2Z cell apoptosis, and the activation of VSOR chloride channels may initiate the GNA-induced apoptosis of CNE-2Z cells. On this basis, this experiment further studies the relationship between the activation of the VSOR Cl^- channel and ER stress-mediated apoptosis in CNE-2Z cells.

Recent years have seen the discovery that the ER stress-mediated apoptosis pathway differs from the mitochondrial pathway and the death receptor in that it can induce apoptosis independently through its own signal transduction pathway. In normal cells, GRP78, ATF6, IRE 1 and PERK form an integrated inactive complex. Under ER stress,

 doi:10.20944/preprints201806.0141.v1

the unfolded protein is increased, and GRP78 is separated from the complex and activated. Then, the signal is transmitted to the nucleus and initiates UPR. RP78 mainly exists in the ER and contributes significantly to the activation of the proto-oncogene. Previous research has found that the expression of GRP78 could be detected on the surfaces of tumor cells instead of normal cells [31]. Thanks to the research progress on the ER stress-related signal pathway, it has been discovered that UPR can induce CHOP transcription by PERK, ATF6 and IRE1. Specifically, the PERK-eIF2a-ATF4 pathway has become a research hotspot and the most important regulator of CHOP [32]. As the main molecular marker of ER stress, CHOP belongs to the C/EBP family of transcription factors. Under normal circumstances, the CHOP content is low in the cytoplasm. However, ER stress can induce the expression of CHOP by regulating the nuclear target gene. CHOP is involved in the regulation of cell survival or apoptosis mediated by ER stress [33]. It is increasingly expressed in the nucleus when ER stress induces apoptosis, and the overexpression could induce cell apoptosis.

It is also meaningful to discuss whether the apoptosis induced by the VSOR Cl^- channel is correlated with the ER pathway. Thus, this study seeks to clarify the intrinsic relationship between the VSOR Cl^- channel and the level of ER stress-related protein. The research results are as follows: the expression of GRP78 protein declines in CNE-2Z cells treated with GNA after 24 h, and the expressions of CHOP and ATF4 proteins increase. This indicates GNA may down-regulate the expression of ER stress-related protein GRP78 and up-regulate the expression of ER stress-related proteins CHOP and

 doi:10.20944/preprints201806.0141.v1

ATF4. In this way, GNA contributes to the unfolded protein response protection mechanism, suppresses the anti-apoptosis effect of UPR, and thereby induces the apoptosis of the NPC cell line CNE-2Z. In contrast, DIDS and DCPIB hinder the cell apoptosis by down-regulating ER stress protein GRP78, up-regulating ATF4 protein, and blocking CHOP. Obviously, DIDS and DCPIB drag down the expression level of GNA-induced apoptosis factor CHOP, suggesting that the VSOR Cl^- channel is engaged in the ER stress-mediated apoptosis of CNE-2Z cells.

5. Conclusions

In summary, GNA induces the apoptosis of CNE-2Z cells through the steps below: it participates in the AVD regulation of early apoptosis events of CNE-2Z cells through activating volume sensitive chloride channels, promoting the increase in the amount of CHOP expression in the nucleus via the activation of UPR through the ER stress pathway, and causing cell apoptosis with the excessive expression of CHOP. In spite of the valuable findings mentioned above, it is necessary to study the role of CHOP signaling molecules in the pathogenesis of the NPC CNE-2Z cell line damage and the function of the downstream signaling molecules.

Acknowledgements: This work was supported by National Natural Science Foundation of China (81673650, 81173600, Q.L) and Key Project of Anhui Natural Science Research (KJ2017A288, H.C)

 doi:10.20944/preprints201806.0141.v1

Author Contributions: Jingjing Su, Ting Xu and Qinglin Li conceived and designed the experiments. Jingjing Su, Ting Xu, Genling Jiang assisted with the experiments. Hui Cheng, Mengru Liang and Mei Hou assisted in the culturing of the cells. Jingjing Su and Ting Xu performed the experiments, analyzed the raw data, and wrote the manuscript. All authors read and approved the final manuscript.

Conflict of interest: The authors declare that there are no conflicts of interest to reveal.

References

1. Wee, J. T. S.; Ha, T. C.; Loong, S. L. E.; Qian, C., Is nasopharyngeal cancer really a "Cantonese cancer"? *Chin. J. Cancer* **2010,** 29, (5), 517-526.
2. Chen, Y.; Sun, Y.; Liang, S. B.; Zong, J. F.; Li, W. F.; Chen, M.; Chen, L.; Mao, Y. P.; Tang, L. L.; Guo, Y.; Lin, A.; Liu Meng Zhong; Ma, J., Progress report of a randomized trial comparing long-term survival and late toxicity of concurrent chemoradiotherapy with adjuvant chemotherapy versus radiotherapy alone in patients with stage III to IVB nasopharyngeal carcinoma from endemic regions of China. *Cancer* **2013,** 119, (12), 2230-8.
3. Liu, X.; Luo, H. N.; Tian, W. D.; Lu, J.; Li, G.; Wang, L.; Zhang, B.; Liang, B. J.; Peng, X. H.; Lin, S. X.; Peng, Y.; Li, X. P., Diagnostic and prognostic value of plasma microRNA deregulation in nasopharyngeal carcinoma. *Cancer Biol. Ther.* **2013,** 14, (12), 1133-42.
4. Chou, J.; Lin, Y. C.; Kim, J.; You, L.; Xu, Z. D.; He, B.; Jablons, M. D., Nasopharyngeal carcinoma--review of the molecular mechanisms of tumorigenesis. *Head Neck* **2008,** 30, (7), 946-63.
5. Li, X. M.; Zhang, K. Z.; Li, Z. H., Unfolded protein response in cancer: the physician's perspective. *J. Hematol. Oncol.* **2011,** 4, 8.
6. Bao, C.; Zhang, J.; Liu, J.; Liu, H.; Wu, L.; Shi, Y.; Li, J.; Hu, Z.; Dong, Y.; Wang, S.; Zeng, X.; Wu, H., Moxibustion treatment for diarrhea-predominant irritable bowel syndrome: study protocol for a randomized controlled trial. *BMC Complement. Altern. Med.* **2016,** 16, (1), 408.
7. Kim, I.; Xu, W. j.; Reed, C. J., Cell death and endoplasmic reticulum stress: disease relevance and therapeutic opportunities. *Nat. Rev. Drug Discov.* **2008,** 7, (12), 1013-30.
8. Chen, L. X.; Zhu, L. Y.; C., J. T. J.; Wang, L. W., Roles of volume-activated Cl – currents and regulatory volume decrease in the cell cycle and proliferation in nasopharyngeal carcinoma cells. *Cell Prolif.* **2007,** 40, 253-267.

9. Zhu, L. Y.; Yang, H. F.; Zuo, W. H.; Yang, L. J.; Zhang, H. F.; Ye, W. C.; Mao, J. W.; Chen, L. X.; Wang, L. W., Differential expression and roles of volume-activated chloride channels in control of growth of normal and cancerous nasopharyngeal epithelial cells. *Biochem. Pharmacol.* **2012,** 83, (3), 324-34.
10. Maeno, E.; Ishizaki, Y.; Kanaseki, T.; Hazama, A.; Okada, Y., Normotonic cell shrinkage because of disordered volume regulation is an early prerequisite to apoptosis. *Proc. Natl. Acad. Sci. U. S. A.* **2000,** 97, 9487-9492.
11. Lee, L. E.; Shimizu, T.; Ise, T.; Numata, T.; Konho, K.; Okada, Y., Impaired Activity of Volume-Sensitive ClS Channel Is Involved in Cisplatin Resistance of Cancer Cells. *J. Cell. Physiol.* **2007,** 211, 513-21.
12. He, W.; Li, H.; Min, X. J.; Liu, J.; Hu, B.; Hou, S. C.; Wang, J., Activation of volume-sensitive Cl-channel is involved in carboplatin-induced apoptosis in human lung adenocarcinoma cells. *Cancer Biol. Ther.* **2010,** 9, 885-891.
13. Akita, T.; Okada, Y., Characteristics and roles of the volume-sensitive outwardly rectifying (VSOR) anion channel in the central nervous system. *Neuroscience* **2014,** 275, 211-31.
14. Pogorelova, M. A.; Golichenkov, V. A.; Pogorelova, V. N.; Panait, A. I.; Smirnov, A. A.; Pogorelov, A. G., Amino Acid Correction of Regulatory Volume Decrease Evoked by Hypotonic Stress in Mouse Oocytes In Vitro. *Bull. Exp. Biol. Med.* **2015,** 159, (1), 35-7.
15. Okada, Y.; Shimizu, T.; Maeno, E.; Tanabe, S.; Wang, X.; Takahashi, N., Volume-sensitive chloride channels involved in apoptotic volume decrease and cell death. *J. Membr. Biol.* **2006,** 209, (1), 21-9.
16. Kumagai, K.; Imai, S.; Toyoda, F.; Okumura, N.; Isoya, E.; Matsuura, H.; Matsusue, Y., 17beta-Oestradiol inhibits doxorubicin-induced apoptosis via block of the volume-sensitive Cl(-) current in rabbit articular chondrocytes. *Br. J. Pharmacol.* **2012,** 166, (2), 702-720.
17. Zhang, Y. M.; Ren, J., Targeting autophagy for the therapeutic application of histone deacetylase inhibitors in ischemia/reperfusion heart injury. *Circulation* **2014,** 129, (10), 1088-91.
18. Dongworth, K. R.; Hall, R. A.; Burke, N.; Hausenloy, J. D., Targeting mitochondria for cardioprotection: examining the benefit for patients. *Future Cardiol.* **2017,** 10, 255-272.
19. Shen, M.; Wang, L.; Wang, B.; Wang, T.; Yang, G.; Shen, L.; Wang, T.; Guo, X.; Liu, Y.; Xia, Y.; Jia, L.; Wang, X., Activation of volume-sensitive outwardly rectifying chloride channel by ROS contributes to ER stress and cardiac contractile dysfunction: involvement of CHOP through Wnt. *Cell Death Dis.* **2014,** 5, e1528.
20. Pedersen, F. S.; Okada, Y.; Nilius, B., Biophysics and Physiology of the Volume-Regulated Anion Channel (VRAC)/Volume-Sensitive Outwardly Rectifying Anion Channel (VSOR). *Pflugers Arch.* **2016,** 468, (3), 371-83.
21. Li, Q. L.; Cheng, H.; Zhu, G. Q.; Yang, L.; Zhou, A.; Wang, X. S.; Fang, N. B.; Xia, L. Z.; Su, J. J.; Wang, M.; Peng, D. Y.; Xu, Q., Gambogenic acid inhibits proliferation of A549 cells through apoptosis-inducing and cell cycle arresting. *Biol. Pharm. Bull.* **2010,** 33, (3), 415-420.
22. Yan, F. G.; Li, Q. L., Gambogenic acid induced apoptosis in human nasopharyngeal carcinoma CNE-1 cells and effect of p-p38 and p-ERK1/2 protein. *Chinese Pharmacological Bulletin* **2011,** 27, 355-359.

23. Yan, F. G.; Wang, M.; Li, J. M.; Cheng, H.; Su, J. J.; Wang, X. S.; Wu, H. Y.; Xia, L. Z.; Li, X. X.; Change, C. H.; Li, Q. L., Gambogenic acid induced mitochondrial-dependent apoptosis and referred to phospho-Erk1/2 and phospho-p38 MAPK in human hepatoma HepG2 cells. *Environ. Toxicol. Pharmacol.* **2012,** 33, (2), 181-90.
24. Chen, H. B.; Zhou, L. Z.; Mei, L.; Shi, X. J.; Wang, X. S.; Li, Q. L., Gambogenic acid-induced time- and dose-dependent growth inhibition and apoptosis involving Akt pathway inactivation in U251 glioblastoma cells. *J. Nat. Med.* **2012,** 66, (1), 62-9.
25. Wang, M.; Chen, D.; Cheng, H.; Li, B.; Yan, F. G.; Su, J. J.; Peng, C.; Sun, M. L.; Hu, Y. W.; Wang, X. S.; Wang, G. H.; Chen, Z. W.; Li, Q. L., Gambogenic Acid Kills Lung Cancer Cells through Aberrant Autophagy. *PLoS One* **2014,** 9, e83604.
26. Yang, X.; Zhu, L.; Lin, J.; Liu, S.; Luo, H.; Mao, J.; Nie, S.; Chen, L.; Wang, L., Cisplatin Activates Volume-Sensitive Like Chloride Channels Via Purinergic Receptor Pathways in Nasopharyngeal Carcinoma Cells. *The Journal of Membrane Biology* **2014,** 248, (1), 19-29.
27. Bo, Z. Q.; Li, H. R.; Zhang, H.; Liu, S. W.; Zhu, L.; Chen, L. X.; Wang, L. W., Role of chloride channels in Gambogic acid-induced apoptosis of poorly differentiated nasopharyngeal carcinoma cells. *J South Med Univ* **2011,** 31, 1304-1308.
28. Cheng, H.; Peng, D. Y.; Wang, X. S.; Tang, L. J.; Huang, P.; Li, Q. l., Antitumor effects of neogambogic acid both in vivo and in vitro. *Chin Tradit Herbal Drugs* **2008,** 39, 236-240.
29. Shimizu, T.; Numata, T.; Okada, Y., A role of reactive oxygen species in apoptotic activation of volume-sensitive Cl(-) channel. *Proc. Natl. Acad. Sci. U. S. A.* **2004,** 101, (17), 6770-3.
30. Mao, J. W.; Chen, L. X.; Xu, B.; Wang, L. J.; Li , H.; Guo, J.; Li, W. D.; Nie , S. H.; Jacob, J. C. T.; Wang, L. W., Suppression of ClC-3 channel expression reduces migration of nasopharyngeal carcinoma cells. *Biochem. Pharmacol.* **2008,** 75, (9), 1706-16.
31. Lin, Y.; Tsai, N. M.; Hsieh, C. H.; Ho, S.; Chang, J.; Wu, H.-Y.; Hsu, M. H.; Chang, C. C.; Liao, K. W.; Jackson, T. L. B.; Mold, D. E.; Huang, R. C. C., In vivo amelioration of endogenous antitumor autoantibodies via low-dose P4N through the LTA4H/activin A/BAFF pathway. *Proc. Natl. Acad. Sci. U. S. A.* **2016,** 113, (48), 7798-7807.
32. Erbay, E.; Babaev, R. V.; Mayers, R. J.; Makowski, L.; Charles, N. K.; Snitow, M.; Fazio, S.; Wiest, M. M.; Watkins, M. S.; Linton, F. M.; Hotamisligil, S. G., Reducing endoplasmic reticulum stress through a macrophage lipid chaperone alleviates atherosclerosis. *Nat. Med.* **2009,** 15, (12), 1383-1391.
33. Ma, J.; Qiu, Y.; Yang, L.; Peng, L.; Xia, Z.; Hou, L. N.; Fang, C.; Qi, H.; Chen, H. Z., Desipramine induces apoptosis in rat glioma cells via endoplasmic reticulum stress-dependent CHOP pathway. *J. Neurooncol.* **2011,** 101, (1), 41-8.